Cement and Concrete Research 38 (2008) 938–944

Contents lists available at ScienceDirect

Cement and Concrete Research

journal homepage: http://ees.elsevier.com/CEMCON/default.asp

Effect of limestone filler BET(H_2O)-area on the fresh and hardened properties of self-compacting concrete

O. Esping

Department of Civil and Environmental Engineering, Chalmers University of Technology, Sweden

ARTICLE INFO

Article history:
Received 21 August 2007
Accepted 12 March 2008

Keywords:
Concrete
Filler
Surface area
Rheology
Autogenous
Shrinkage

ABSTRACT

This paper presents a study on the use of limestone fillers with different specific surface area and their effect on the fresh and hardened properties of self-compacting concrete (SCC). The surface area was determined by a simplified BET method using water vapour as adsorbate. A rheometer and a slump flow test were used to measure the flowability of fresh concrete. A concrete dilatometer was used to measure the autogenous shrinkage, and a ring-test for the plastic cracking tendency. The compressive strength was determined at 28 days. It was found that the measure of BET(H_2O)-area can be used to evaluate the water requirement for constant workability of the SCC, where a change in BET(H_2O)-area of 1000 m^2/kg corresponds to approximately 0.8% in moisture content. The results showed that filler with a large area will result in an increased autogenous shrinkage, decreased evaporation, lower plastic cracking tendency, and a higher compressive strength. With additional water the results was the opposite.

1. Introduction

Ground limestone has been used in concrete production for the last 25 years [1], not only for the main purposes of lowering the costs and environmental load of cement production, but also to increase the concrete durability. More recently ground limestone is also used as a filler material to improve the workability and stability of fresh concrete. For a high flowable concrete, such as self-compacting concrete (SCC), limestone filler is added to increase the packing of the granular skeleton, bind (physically) excess water and increase the volume of the continuous phase of lubricating paste. SCC has to possess two incompatible properties: high flowability and high segregation resistance. This balance is made possible by the dispersing effect of high-range water-reducing admixture (superplasticizer) combined with cohesiveness of high concentration of fine particles in additional filler material [2]. The main mechanisms controlling this fine balance are related to surface physics and chemistry; hence SCC is strongly dependent on surface activity of the admixtures together with the high specific surface area generated by the fines [3]. A consequence of the high concentration of powder material and the retarding effect of superplasticizer, the concrete may develop a large autogenous shrinkage and plastic cracking tendency [4]. At early age, when the cement paste is young and has poorly developed mechanical properties, evaporation and autogenous shrinkage, both incorporated in the plastic shrinkage, are the two main driving forces for cracking. When the concrete dries out, the loss of water from the paste generates negative capillary pressure, causing the paste to contract, which in turn can lead to cracks [5]. These contracting capillary forces are in reverse proportional to the meniscus radius, and hence the capillary tension stresses increase with decreasing pore sizes and interparticle spaces. For a concrete where evaporation is prevented, a contracting negative capillary pressure will also develop, but only when the hydration commences and the concrete sets [6]. As long as the concrete is fluid, autogenous shrinkage is generally considered to be equal to the chemical shrinkage; but once the self-supporting skeleton starts to form, the autogenous will diverge from the chemical [7,8]. The setting will be manifested as a change of the slope of the autogenous deformation, and once the internal voids are created the development of capillary pore underpressure in the skeletal structure will cause an external deformation [9]. The pattern of autogenous deformation, exampled in Fig. 1, comprises three distinct stages which can be defined as plastic, semiplastic and rigid, separated by the time to initial and final set [9,10].

The physical nature of better packing, by addition of filler material, will not only govern the concrete flowability, but also the compressive strength due to the denser matrix and the better dispersion of cement grains [12–15]. Furthermore, the surfaces of the filler material will act as nucleation sites for the early reaction products of CH and CSH, which will accelerate the hydration of cement clinkers (especially C_3S) and consequently increase the early age compressive strength [16–19]. The effect of nucleation on the strength is dependent on the filler's affinity to cement hydrates, and it increases with fineness and specific

E-mail address: oskar.esping@bt.chalmers.se.

0008-8846/$ – see front matter © 2008 Elsevier Ltd. All rights reserved.
doi:10.1016/j.cemconres.2008.03.010

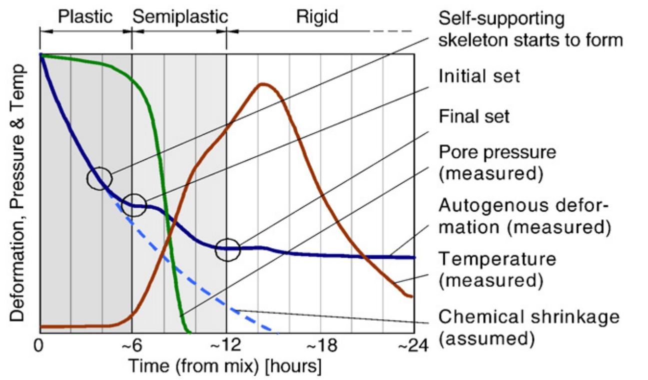

Fig. 1. Typical early-age linear autogenous deformation and corresponding development of temperature and capillary pore pressure (based on measures of a SCC w/c 0.45, from [11]).

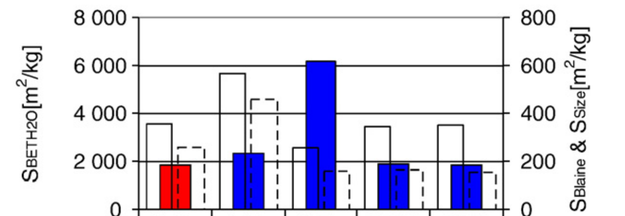

	L40	L15	L70	G100	G200
BET(H2O)	1808	2307	6148	1894	1821
Blaine	357	565	254	345	353
Size	259	458	160	165	154

Fig. 2. The five limestone fillers' specific surface area by BET(H_2O) and by Blaine, and calculated from size distribution.

surface area of the filler. Limestone filler is not pozzolan, but nor fully inert as it reacts with the alumina phases of the cement. If the cement has a significant amount of tricalcium aluminate (C_3A), calcium carboaluminate will be produced from the reaction between calcium carbonate ($CaCO_3$) from the limestone and the C_3A [20–26]. This reaction, accelerating the hydration and increasing the compressive strength, increases with the C_3A content of the cement and the fineness and specific surface area of the filler.

Since the ratio of surface area to volume increases exponentially with particle irregularity (shape, texture and porosity) and decreased size, and as this area has a predominating effect on fresh and hardened concrete [27–30], quantification of geometrical properties of fillers and fines is essential. Powder material (filler, cement, etc.) is traditionally characterized by the size distribution and the specific surface area by Blaine fineness. Due to the methodology where the specific surface area is determined from air permeability, based on packed spherical particles, information about the shape, texture and surface porosity is neglected [27,31]. Other possibly more correct methods, such as the BET with nitrogen gas and image analysis, are more seldom used due to their complexity and costs.

In this work, the effect of the specific surface area of different limestone fillers on the fresh and hardened properties of self-compacting concrete (SCC) has been experimentally evaluated. The investigated properties were rheology, autogenous deformation, plastic cracking tendency and compressive strength. The surface area was determined by a simplified BET method, using water vapour as adsorbate. The change in BET(H_2O)-area was translated to a change in water demand for the concrete mix to maintain a constant workability, based on the assumption that 30 full molecular layers of water covering the particle surface are required to decrease interactions and provide sufficient lubrication for flowability.

2. Materials and mix design

The mix design and its constituents, as used in this study, comprise typical materials and compositions for self-compacting concrete with w/c 0.55 in Sweden. The cement was a type CEM II/A-LL 42.5R, the fine aggregate a 0–8 mm natural pit gravel, the coarse aggregate a 8–16 mm crushed granite stone and the superplasticizer a polycarboxylate ether-based type. Five ground limestone fillers, with similar chemical composition but different size distributions and specific surface areas, were used. The area was determined by BET(H_2O); A simplified method, based on the BET theory [32], where the area was determined gravimetrically on conditioned samples at different relative humidities and deduced from the adsorbed volume of water molecules required to cover and form a monolayer on the surface of the sample [27,33–36]. The measured BET(H_2O)-area (S_{BETH2O}), the area by Blaine (S_{Blaine}) and the calculated area from size distribution (S_{Size}) [33,36] for the five limestone fillers are given in Fig. 2. The size distribution, measured with a Malvern laser diffraction instrument, is presented in Fig. 3. The limestone filler named L40 has the smallest BET-area, and is used as a reference. It can be noted that the filler named L70 is the coarsest, but has the largest BET-area.

The BET(H_2O)-area for the gravel is ~2800 m^2/kg, and the BET(N_2)-area for the cement is ~2000 m^2/kg. For cement the BET(H_2O) method is not valid. Due to the differences in size and polarity of the water and nitrogen molecule the area by BET(H_2O) is larger than by BET(N_2) [36]. With a linear relationship of 1.55 [11], the BET(H_2O)-area for the cement can be estimated to 3100 m^2/kg.

Corresponding mixtures were made without the presence of cement, in order to evaluate the effect (if any) of fillers' surface area on the autogenous deformation without influence of chemical shrinkage. The cement content (340 kg/m^3) was replaced with an equal volume of limestone filler (i.e. filler content increased from 160 to 458 kg/m^3), whereas the other constituents was kept constant.

Finally, mixtures were made with additional water, compensating for the fillers' differences in BET(H_2O)-area in order to regain constant flowability. A model was used where 30 molecular layers of water covering the particle surface are required to decrease interactions and provide lubrication sufficient to create flowability [27]. An increase in BET(H_2O)-area of 1000 m^2/kg corresponds to a need for additional water of ~0.8% by mass of filler (or gravel) content for constant flowability. In Table 1 the changes in mixing water due to differences in specific area of limestone filler, using L40 as reference, are given. The fillers were selected due to their difference in size distribution, not BET-area. As G200 provided similar area as L40, the compensation in mixing mater was rather limited for G200 mix.

The concrete was prepared in batches of 40 l, and mixed in a BHS-60 twin-shaft paddle mixer for 4 min after water was added to the

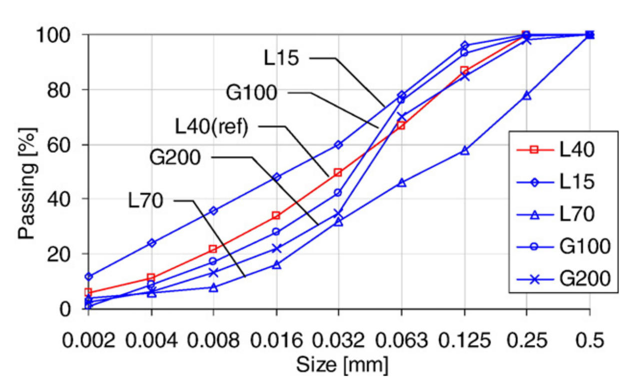

Fig. 3. Size distributions for the five limestone fillers'.

Table 1
Mixing water, in litre/m^3, with compensations for the differences in specific surface area of limestone fillers

L40 (ref)	L15	L70	G100	G200
187.00	187.68 (+0.68)	192.89 (+5.89)	187.12 (+0.12)	187.02 (+0.02)

The L40 with the smallest BET-area is used as reference.

premixed dry materials. The admixtures were added directly after the water.

3. Experimental methods

3.1. Flowability test methods

A slump flow test was carried out by using a traditional slump cone (EN 12350-2), measuring the spread flow diameter (average from two perpendicular directions).

Concrete rheology measurements were performed using a ConTec Visco5 with a rotating concentric setup at a controlled shear rate ($\dot{\gamma}$). The experimental geometry and measuring sequence are illustrated in Fig. 4. The rheological parameters, plastic viscosity (η_{pl}) and yield stress (σ_0), were evaluated in accordance with the Bingham model:

$$\sigma = \sigma_0 + \dot{\gamma} \cdot \eta_{pl} \tag{1}$$

Both slump flow and the rheology test were performed at 7 and 60 min after adding water to mix.

3.2. Autogenous deformation test method

The autogenous linear deformation was monitored by a concrete digital dilatometer (CDD), able to measure before setting when concrete is fresh [11]. The method is a modification of the CT1 dilatometer for pastes and mortars by Jensen and Hansen [37]. The CDD setup consists of a concrete specimen cast in a steel coil-reinforced vapour-proof flexible PE-tube with tight end-caps, a measuring rig in stainless steel, and a digital gauge (3 µm accuracy) recording the unrestrained linear deformation; see Fig. 5. The test, containing three complete CDD setups, was performed at 20±1 °C, and was started at 30 min from water addition.

Due to greater stiffness in the radial than in the longitudinal direction of the mould, in fluid state, the flexible mould transforms a large part of the volumetric deformation into a linear deformation. As the concrete undergoes transition from a fluid to a rigid state, the deformation becomes isotropic. Based on empirical evaluation, the ratio between linear and volumetric deformation for a liquid is approximately 0.8 [38]. No correction for this was made as the setting point is not a well-defined physical state but rather a continuous transformation from liquid to a solid state.

The experiments were supplemented with measurements of temperature and pore pressure placed in the centre of the core. The pressure transducers were connected to a de-aired water-filled system with a needle (internal diameter of 0.4 mm and 50 mm length).

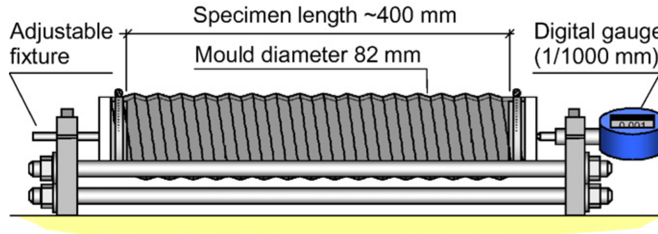

Fig. 5. The concrete digital dilatometer (CDD) for linear autogenous deformation measurement (from [11]).

3.3. Ring-test method for plastic shrinkage cracking

The plastic cracking tendency of concrete at early ages exposed to drying was evaluated, using a modified ring-test method [11], originally developed by Johansen and Dahl [39]. In the test, the fresh concrete is cast between two concentric steel rings and then exposed to drying; see Fig. 6. The measurement was started at 60 min after water addition, and the sample was exposed to an air velocity of 4.5 m/s with 23±2 °C and 35±5% RH. Temperature, pore pressure and weight loss (evaporation) in the concrete specimens, and the strain in the inner ring, were continuously recorded. After 20 h of drying the crack index was measured as the average (of three specimens) total crack area (crack length×crack width) on the concrete surface. The crack width was measured with a crack microscope, and the length with a digital measuring wheel.

3.4. Compressive strength test

Compressive strength was measured on 150 mm cubes after 28 days, in accordance with EN 12390-1,-2 and -3. All presented values of compressive strength (f_c) are normalized to a porosity of 4%. Due to the differences in limestone fillers' BET-area the flowability was not consistent between the mixtures; hence also the air content was not equal. A series of corresponding mixes with different air content, in the range of 0–5%, were made in order to evaluate the effect of air

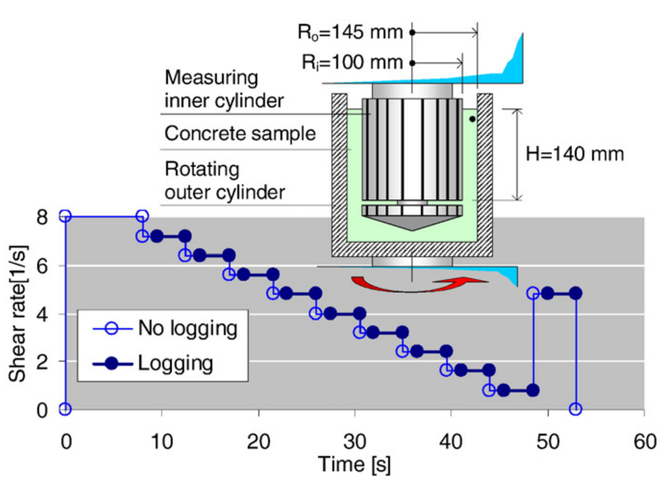

Fig. 4. The ConTec Visco5 geometry, and the measuring sequence for the Bingham evaluation and segregation estimation (from [27]).

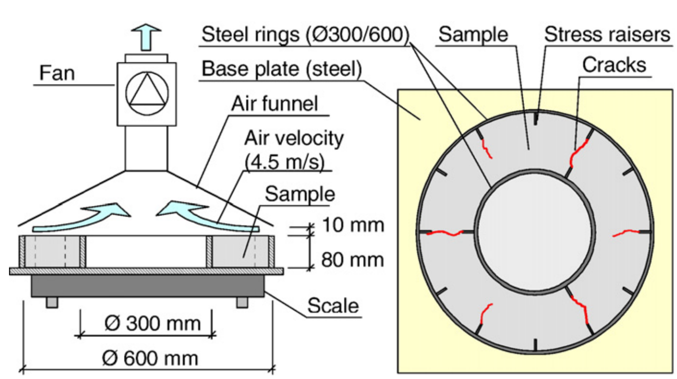

Fig. 6. The ring-test method for evaluation of plastic shrinkage crack tendency (from [11]).

content (porosity) on the compressive strength. This was made in accordance with the general equation for ceramic materials [40]:

$$f_c = f_{c0} \cdot e^k \cdot P \qquad (2)$$

The air content (i.e. porosity), P, was determined by the measured density in fresh and hardened states (according to EN 12350-6 and EN 12390-7), together with the measured air content by pressure test (EN 12350-7). The compressive strength "without" pores, f_{c0}, was 55.0 MPa for the concrete de-aired in a vacuum desiccator for 30 min before moulding. The constant k was empirically evaluated to 6.5.

4. Results and discussion

All test results are represented by a mean value based on two or more tests. For more details see [41,42].

4.1. Flowability

The results from the concrete flowability measurements (slump flow, yield stress and plastic viscosity) are presented in Fig. 7.

The results shows that the limestone filler BET(H_2O)-area have a strong influence on the SCC flowability. The larger area, the higher yield stress and viscosity, and consequently the lower slump flow. The loss in flowability by time is significant regarding slump flow and yield stress, and increases with BET(H_2O)-area, whereas the change in viscosity by time is small.

Furthermore, results indicated that the differences in BET(H_2O)-area can be compensated for with a calculated change in water content in order to regain constant flowability. All mixtures with additional water showed nearly the same rheological measures as the reference mix with "L40". At 7 min the slump flow for the reference SCC (L40) and the mixtures with additional water was 595 ± 5 mm, the yield stress 71 ± 12 Pa, and the viscosity 35 ± 2 Pa s. The deviations were similar for the measures at 60 min. The results are presented in [41], and also confirmed by similar tests with natural gravel with different BET-area.

The specific area by Blaine and from size distribution (see Fig. 2) showed a poor correlation with the flowability, which can be explained by the differences in size distribution (see Fig. 3). Thus, despite that "L70" is coarse, it generates a larger specific area and thereby a stiffer consistency, and has a larger water demand. This might be explained by the filler's geological origin and age, where "L70" has a rougher and more porous particle surface.

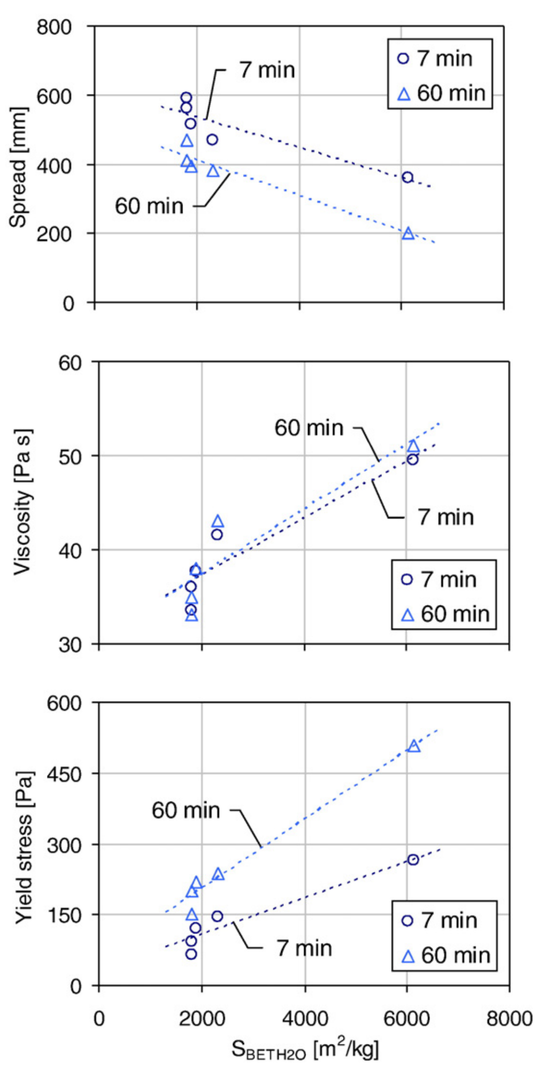

Fig. 7. Limestone fillers BET(H_2O)-area vs. slump flow, yield stress and plastic viscosity for the SCC mixtures (at 7 and 60 min), and a suggested linear tendency.

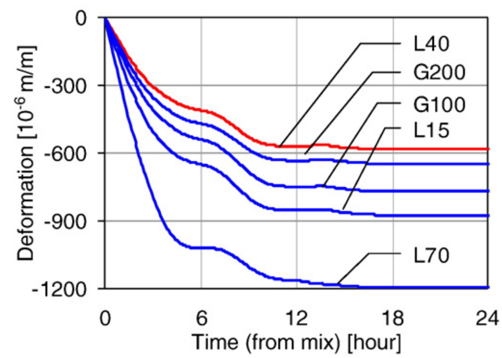

Fig. 8. Autogenous deformation for the SCC with different limestone fillers (from [42]).

4.2. Autogenous deformation

The results (from [42]) of the autogenous deformation measurements are presented in Fig. 8, and the evaluated rate of deformation in Fig. 9. As can be observed, increased surface area by BET(H_2O) increased both the magnitude and rate of shrinkage, primarily in the plastic region. The time to initial and final set were 6.1 and 11.6 h from mix respectively. The time of set is where the rate of autogenous deformation reaches a minimum, see Fig. 1. The differences in BET-area had almost no effect on times to set (shorter than ±0.1 h). This was

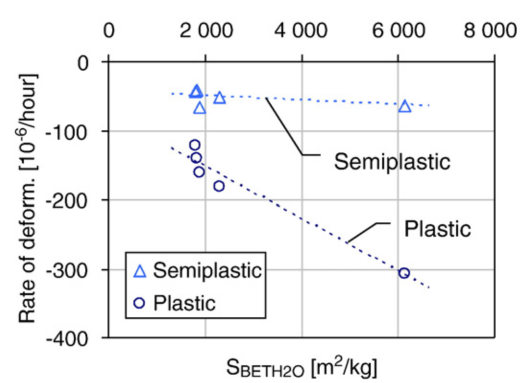

Fig. 9. The limestone filler's BET(H_2O)-area and the evaluated rate of autogenous deformation from autogenous deformation in the plastic and semiplastic period, and a suggested linear tendency.

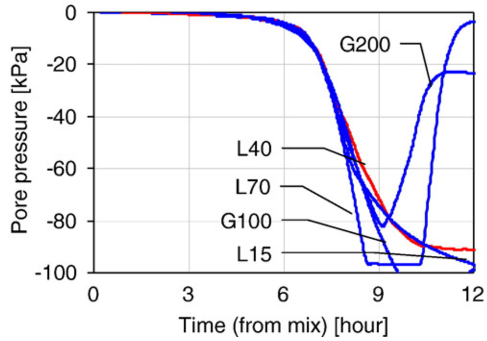

Fig. 10. Development of capillary pore pressure during the first 12 h from water addition (from [42]).

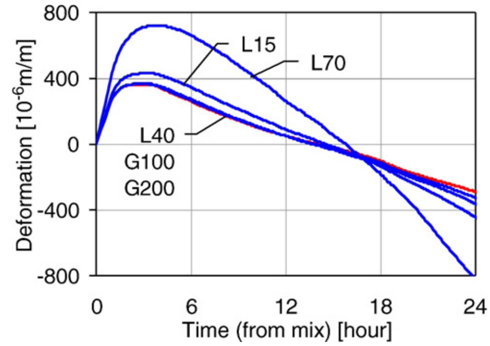

Fig. 12. Sealed ("autogenous") deformation for the mixtures where the cement was replaced with equal-volume filler (from [42]).

confirmed by the measured temperature development, showing almost no differences.

Previous tests show that increased water content decreases the rate and magnitude of autogenous deformation, without affecting the time to set, which is equivalent to the effect of decreased particle surface area [11].

Furthermore, Fig. 10 shows the development of the measured pore pressure, and Fig. 11 the evaluated maximum rate of pore pressure which occurred at 7–8 h from mixing [42]. The point of maximum underpressure could not be evaluated due to the loss of pressure at random times. This effect is usually referred to as the breakthrough pressure [5]. It can be noted that the rate of pore pressure, and rate and magnitude of autogenous deformation, showed to correlate with the limestone fillers' BET(H_2O)-area.

The results of the measured "autogenous" deformation for the mixtures without cement (same composition, but cement is replaced with equal-volume limestone filler) are presented in Fig. 12. There was no separation observed, thus no cement was present, and the consistencies were similar to the corresponding SCC mixtures.

The hydration process (generating chemical shrinkage) is generally considered to be the driving force of autogenous deformation; hence the term "autogenous" in this case might be incorrect. Even though no cement is present, the mixes generated an "autogenous" shrinkage of approximately 0.8 mm/m at 24 h, counted after an initial swelling up to 4 h. This is the same magnitude as for the mixes with cement, but those generated no swelling and almost all shrinkage before final set. At 48 h, the development of shrinkage levels out. It ought to be noted that the effect of differences in surface area is augmented, as the content of limestone filler is larger relative to the SCC mixtures (i.e. 458 instead of 160 kg/m^3). The results indicate that larger BET(H_2O)-area increases the deformation (both swelling and shrinkage). The expansion can be explained by water being absorbed by the filler (and aggregate) and by the disjoining pressure, i.e. the adsorption of water molecules in locations where the distance between two surfaces is restricted, inducing pressure and expansion [43]. Once lack of water occurs, this causes a restraining matrix of particles, and there will be pores with meniscus-generated capillary tension and thereby a contraction [44].

4.3. Plastic shrinkage cracking

A representative measure (from [42]) showing the relationship between the development of strain, temperature, and pore pressure (at 20 and 60 mm depth) for one of the concretes exposed to drying is shown in Fig. 13. As can be seen, the pore pressure develops more rapidly in comparison with the sealed samples, in Fig. 10. The maximum underpressure is reached at 5–6 h from mix, with approximately 30 min between the two depths. The measured strains indicate that cracking was initiated at 3–4 h from mixing [42]. The average crack area is presented in Fig. 14, where it can be seen that the crack tendency is lower for concrete incorporating filler with a high BET (H_2O)-area, and that, when adding extra water to compensate for the loss in flowability, the crack tendency increased significantly. With an assumed linear relationship, an increase in filler's BET(H_2O)-area of 1000 m^2/kg results in ~20% less cracking tendency.

The differences in crack tendency are most likely a consequence mainly of evaporation, which is verified by the initial rate of measured evaporation (up to 4 h from mix, before initial setting) in Fig. 15. A large particle surface area lowers the evaporation, whereas extra water increases the evaporation.

4.4. Compressive strength

The results (from [41]) of the measured compressive strength are presented in Fig. 16. Due to the differences in air content, the presented values are adjusted to an equal porosity of 4%, in accordance with Eq. (2). All test results are represented by a mean value based on two or more mixtures.

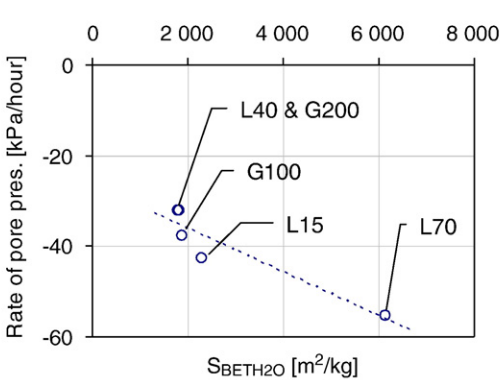

Fig. 11. The limestone filler's BET(H_2O)-area and the evaluated maximum rate of pore pressure (at 7–8 h from mixing), and a suggested linear tendency.

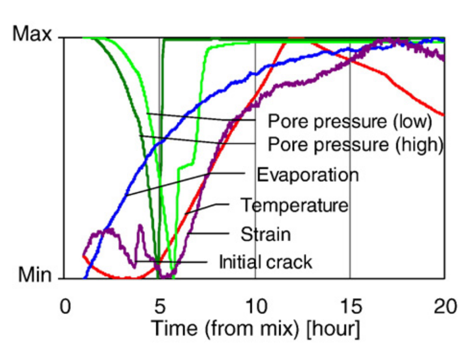

Fig. 13. Development of pore pressure, evaporation, temperature and strain (normalized against maximum values), for the SCC with limestone filler L40 (from [42]).

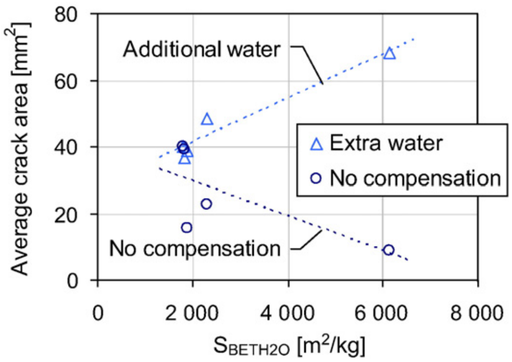

Fig. 14. The limestone filler's BET(H_2O)-area and the plastic shrinkage crack area, without and with extra water compensating for the differences in BET-area ("L40" as reference), and a suggested linear tendency.

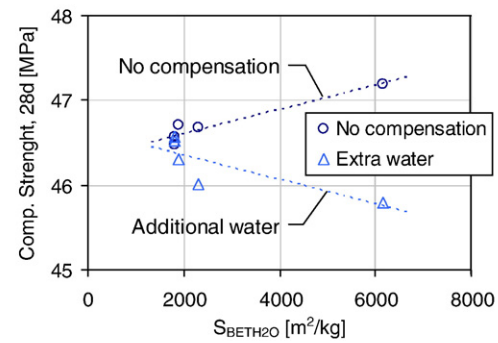

Fig. 16. The limestone filler's BET(H_2O)-area and the SCC compressive strength (28 days), both without and with the extra water added to compensate for the BET (H_2O)-area, and a suggested linear tendency.

As can be observed, the compressive strength increased with BET (H_2O)-area of the filler. For the mixtures with additional water, compensating for the loss in flowability, the effect was the opposite. The increased strength with particle surface area can be attributed to the filler effect (denser packing and accelerated hydration due to nucleation [12–19]). But as the filler with the largest area ("L70") also was the coarsest, the increased strength can also be attributed to the filler's porosity increasing its absorption of water and consequently reducing the effective water/cement ratio. With an assumed linear relationship, a change in BET(H_2O)-area by 1000 m^2/kg correspond to ~0.15 MPa in compressive strength for a SCC with 160 kg limestone fillers (i.e. ~1 kPa/kg filler).

That not only the external surface (accessible to adsorption), but the internal porosity (accessible to water absorption) is incorporated in the BET-area is confirmed by the measured "autogenous" deformation on the mixtures without cement (Fig. 12), where the mixture with "L70" generated the largest shrinkage (and swelling).

5. Conclusions

This paper has presented an experimental investigation of the effect of the specific surface area of five different commercial limestone fillers and their influence on the fresh and hardened properties of self-compacting concrete (SCC). The area was measured with BET(H_2O), a simplified BET method using water (moisture) as adsorbate. Based on the experimental conditions and results in this study, the following observations and conclusions were made:

○ For better control and prediction of fresh and hardened concrete behaviour, the specific surface area by BET is proposed as a potential means of geometrical characterization for fillers.

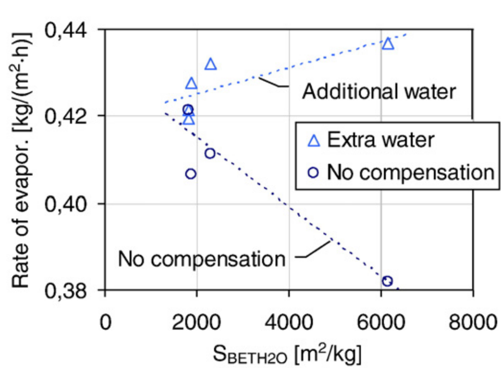

Fig. 15. Initial rate (<4 h from mix) of evaporation, without and with extra water added to compensate for the BET(H_2O)-area, and a suggested linear tendency.

○ Coarser filler can provide larger surface BET-area than finer filler, due to differences in surface texture and accessible porosity.

○ Limestone filler with larger BET(H^2O)-area will decrease the SCC flowability, increase the autogenous shrinkage, decrease the evaporation and thus lower plastic cracking tendency, and generate a higher compressive strength.

○ An increase in BET(H^2O)-area of 1000 m^2/kg corresponds to a need for additional water of ~0.8% by mass of filler content for constant flowability.

○ For a SCC with 160 kg limestone filler, an increase in filler's BET (H^2O)-area of 1000 m^2/kg results in a ~20% lower plastic cracking tendency.

○ With additional water for constant flowability, compensating for the differences in the filler's BET(H^2O)-area, evaporation and plastic cracking tendency was increased, and strength was reduced. The effect of BET(H^2O)-area on the cracking tendency and strength, with additional water, are in reverse ratio to the effect without compensation.

○ The mixtures where the cement was replaced with limestone filler generated an "autogenous" shrinkage of ~0.8 mm/m at 24 h, counted after an initial swelling up to 4 h. The magnitude of deformation (both swelling and shrinkage) corresponded to the limestone filler's BET(H^2O)-area.

References

[1] M. Nehdi, S. Mindess, P.C. Aïtcin, Use of ground limestone in concrete — a new look, Build. Res. J. 43 (1995) 245–261.
[2] H. Okamura, M. Ouchi, Self-compacting concrete. Development, present use and future, Proc. of 1st Int. Symp. on SCC, Stockholm, 1999, pp. 3–14.
[3] Rilem Technical Committee, Final report of Rilem TC 188-CSC Casting of self-compacting concrete, Mat. Struct. 2006).
[4] Ø. Bjøntegaard, T.A. Hammer, E.J. Sellevold, Cracking in high performance concrete before setting, Proc. of Int. Symp. on High Performance and Reactive Powder Concretes, Sherbrooke, 1998.
[5] F.H. Wittmann, On the action of capillary pressure in fresh concrete, Cem. Concr. Res. 6 (1976) 49–56.
[6] E.E. Holt, Early age autogenous shrinkage of concrete, Tech. Res. Centre of Finland, VTT Publ. 446, Finland, 2001.
[7] T.A. Hammer, Test method for linear measurements of autogenous shrinkage before setting, Autogenous shrinkage of concrete, E & FN Spon, London, 1998, pp. 143–154.
[8] O.M. Jensen, F. Hansen, Autogenous deformation and RH-change in perspective, Cem. Concr. Res. 31 (2001) 1859–1865.
[9] L. Barcelo, M. Moranville, B. Clavaud, Autogenous shrinkage of concrete: a balance between autogenous swelling and self-desiccation, Cem. Concr. Res. 35 (2005) 177–183.
[10] A. Radocea, A Study on the Mechanisms of Plastic Shrinkage of Cement-Based Materials, Doctoral thesis, Chalmers, Göteborg, 1992.
[11] O. Esping, I. Löfgren, Cracking due to plastic and autogenous shrinkage — investigation of early age deformation of self-compacting concrete, Publ. 05:11, Chalmers Univ. Tech., Göteborg, 2005.
[12] P. Billberg, Influence of filler characteristics on SCC rheology and early hydration, Proc. 2nd Int. Symp. on SCC, Japan, 2001, pp. 285–294.
[13] V.L. Bonavetti, H. Donza, G. Menéndez, O. Cabrera, E.F. Irassar, Limestone filler cement in low w/c concrete: a rational use of energy, Cem. Concr. Res. 33 (2003) 865–871.

[14] M. Nehdi, S. Mindess, P.-C. Aïtcin, Rheology of high-performance concrete: effect of ultrafine particles, Cem. Concr. Res. 28 (1998) 687–697.
[15] A. Yahia, M. Tanimura, Y. Shimoyama, Rheological properties of highly flowable mortar containing limestone filler-effect of powder content and W/C ratio, Cem. Concr. Res. 35 (2005) 532–539.
[16] P. Lawrence, M. Cyr, E. Ringot, Mineral admixtures in mortars effect of type, amount and fineness of fine constituents on compressive strength, Cem. Concr. Res. 35 (2005) 1092–1105.
[17] A. Nomat, Interactions between chemical evolution (hydration) and physical evolution (setting) in the case of tricalcium silicate, Mat. Struct. 27 (1994) 187–195.
[18] M. Sari, E. Prat, J.K. Labastire, High strength self-compacting concrete — original solutions associating organic and inorganic admixtures, Cem. Concr. Res. 29 (6) (1999) 813–818.
[19] I. Soroka, N. Setter, The effect of fillers on strength of cement mortars, Cem. Concr. Res. 7 (1977) 449–456.
[20] V.L. Bonavetti, V.F. Rahhal, E.F. Irassar, Studies on the carboaluminate formation in limestone filler-blended cements, Cem. Concr. Res. 31 (2001) 853–859.
[21] K.D. Ingram, K.E. Daugherty, A review of limestone addition to Portland cement concrete, Cem. Concr. Comp. 13 (1991) 165–170.
[22] J. Péra, S. Husson, B. Guilhot, Influence of ground limestone on cement hydration, Cem. Concr. Comp. 21 (1999) 99–105.
[23] I. Soroka, N. Stern, Calcareous fillers and the compressive strength of Portland cement, Cem. Concr. Res. 6 (1976) 367–376.
[24] H.F.W. Taylor, Cement Chemistry, Academic Press (2nd Ed), London, 1997.
[25] S. Tsivilis, E. Chaniotakis, E. Badogiannis, G. Pahoulas, A. Ilias, A study on the parameters affecting the properties of Portland limestone cements, Cem. Concr. Comp. 21 (1999) 107–116.
[26] T. Vuk, V. Tinta, R. Gabrovek, V. Kaui, The effects of limestone addition, clinker type and fineness on properties of Portland cement, Cem. Concr. Res. 31 (2001) 135–139.
[27] O. Esping, Rheology of cementitious materials: effects of geometrical properties of filler and fine aggregate, Chalmers Univ. Tech., Göteborg, 2004.
[28] C.F. Ferraris, H.O. Karthik, H. Russell, The influence of mineral admixtures on the rheology of cement paste and concrete, Cem. Concr. Res. 31 (2001) 245–255.
[29] J.L. Gallias, The effect of fine mineral admixtures on water requirement of cement pastes, Cem. Concr. Res. 30 (2000) 1543–1549.
[30] T.C. Powers, The Properties of Fresh Concrete, John Wiley & Sons, New York, 1968.
[31] J.H. Potgier, C.A. Strydom, An investigation into the correlation between different surface area determination techniques applied to various limestone-related compounds, Cem. Concr. Res. 26 (1996) 1613–1617.
[32] S. Brunauer, H.P. Emmet, E. Teller, Adsorption of gases in multimolecular layers, Am. Chem. Soc. (1938).
[33] L. Ahlgren, Moisture fixation in porous building materials, Lund Univ. Tech., Rep. 36, Sweden (in Swedish), 1972.
[34] T. Allen, Particle Size Measurement — Surface Area and Pore Size Determination, Chapman and Hall, London, 1997.
[35] S. Brunauer, The Adsorption of Gases and Vapours, vol. 1, Oxford University Press, Oxford, 1944.
[36] S.J. Gregg, K.S.W. Sing, Adsorption, Surface Area and Porosity, Academic Press, New York, 1967.
[37] O.M. Jensen, F. Hansen, A dilatometer for measuring autogenous deformation in hardening Portland cement paste, Mat. Struct. 28 (1995) 406–409.
[38] O. Esping, I. Löfgren, Investigation of early age deformation in self-compacting concrete, Conf. Advanced Cement-based Materials, DTU, Copenhagen, 2005.
[39] R. Johansen, P.A. Dahl, Control of plastic shrinkage of cement, 18th Conference on Our World in Concrete and Structures, Singapore, 1993.
[40] A.M. Neville, Properties of Concrete, 4th Ed. Pearson Educion Limited, 2000.
[41] O. Esping, SCC flowability: effect of changes in particle surface area, and how to compensate for this, 5th Int. RILEM Symp. on Self-Compacting Concrete, Ghent, 2007.
[42] O. Esping, Investigation of autogenous deformation in self-compacting concrete, RILEM Conf. on Volume Changes of Hardening Concrete, Lyngby, 2006, pp. 273–282.
[43] T. Nawa, T. Horita, Autogenous shrinkage of high-performance concrete, Proc. on microstructure and durability to predict service life of concrete structures, Japan, 2004.
[44] T.A. Hammer, Is there a relationship between pore water pressure and autogenous shrinkage — Before and During Setting? Self-desiccation and its importance in concrete technology, Lund Univ. Tech., TVBM-3104, 2002, pp. 27–38.